

| REPORT DOCUMENTATION PAGE | | | Form Approved OMB NO. 0704-0188 | |
|---|-------------|----------------------------|--|---------------------------------|
| <p>The public reporting burden for this collection of information is estimated to average 1 hour per response, including the time for reviewing instructions, searching existing data sources, gathering and maintaining the data needed, and completing and reviewing the collection of information. Send comments regarding this burden estimate or any other aspect of this collection of information, including suggestions for reducing this burden, to Washington Headquarters Services, Directorate for Information Operations and Reports, 1215 Jefferson Davis Highway, Suite 1204, Arlington VA, 22202-4302. Respondents should be aware that notwithstanding any other provision of law, no person shall be subject to any penalty for failing to comply with a collection of information if it does not display a currently valid OMB control number.</p> <p>PLEASE DO NOT RETURN YOUR FORM TO THE ABOVE ADDRESS.</p> | | | | |
| 1. REPORT DATE (DD-MM-YYYY) | | 2. REPORT TYPE | | 3. DATES COVERED (From - To) |
| | | New Reprint | | - |
| 4. TITLE AND SUBTITLE Isostaticity in Cosserat continuum | | | 5a. CONTRACT NUMBER | |
| | | | W911NF-11-1-0175 | |
| | | | 5b. GRANT NUMBER | |
| 6. AUTHORS Antoinette Tordesillas, Jingyu Shi, John F. Peters | | | 5c. PROGRAM ELEMENT NUMBER | |
| | | | 611102 | |
| | | | 5d. PROJECT NUMBER | |
| 7. PERFORMING ORGANIZATION NAMES AND ADDRESSES University of Melbourne Melbourne Research Swanston Street | | | 5e. TASK NUMBER | |
| | | | 5f. WORK UNIT NUMBER | |
| | | | 8. PERFORMING ORGANIZATION REPORT NUMBER | |
| 9. SPONSORING/MONITORING AGENCY NAME(S) AND ADDRESS(ES) U.S. Army Research Office P.O. Box 12211 Research Triangle Park, NC 27709-2211 | | | 10. SPONSOR/MONITOR'S ACRONYM(S) ARO | |
| | | | 11. SPONSOR/MONITOR'S REPORT NUMBER(S) 58763-EG.2 | |
| 12. DISTRIBUTION AVAILABILITY STATEMENT Approved for public release; distribution is unlimited. | | | | |
| 13. SUPPLEMENTARY NOTES The views, opinions and/or findings contained in this report are those of the author(s) and should not be construed as an official Department of the Army position, policy or decision, unless so designated by other documentation. | | | | |
| 14. ABSTRACT Under conditions of isostaticity in granular media, the contact forces for all particles are statically determinate and forces can be computed without recourse to deformation equations or constitutive relationships. Given that stresses represent spatial averages of inter-particle forces, the stress-equilibrium equations for the isostatic state form a hyperbolic system of partial differential equations that describe the internal stress state using only boundary tractions. In this paper, we consider a Cosserat medium and propose closure relationships in terms of stresses and | | | | |
| 15. SUBJECT TERMS Isostaticity, Cosserat, Granular, Force chains | | | | |
| 16. SECURITY CLASSIFICATION OF: | | 17. LIMITATION OF ABSTRACT | 15. NUMBER OF PAGES | 19a. NAME OF RESPONSIBLE PERSON |
| a. REPORT | b. ABSTRACT | c. THIS PAGE | | Antoinette Tordesillas |
| UU | UU | UU | | 19b. TELEPHONE NUMBER |
| | | | | 038-344-9685 |

Report Title

Isostaticity in Cosserat continuum

ABSTRACT

Under conditions of isostaticity in granular media, the contact forces for all particles are statically determinate and forces can be computed without recourse to deformation equations or constitutive relationships. Given that stresses represent spatial averages of inter-particle forces, the stress-equilibrium equations for the isostatic state form a hyperbolic system of partial differential equations that describe the internal stress state using only boundary tractions. In this paper, we consider a Cosserat medium and propose closure relationships in terms of stresses and couple stresses from observations of stress variations in the critical state regime from discrete element simulations and experiments on sand, even though the isostatic condition is only satisfied in an average sense. It is shown that the governing equations are hyperbolic, which can be solved using the method of characteristics. Examples of both analytic and numerical solutions are presented. These examples clearly demonstrate that stress chains (characteristic lines) form oblique angles with the assumed direction of the force chains.

REPORT DOCUMENTATION PAGE (SF298)
(Continuation Sheet)

Continuation for Block 13

ARO Report Number 58763.2-EG

Isostaticity in Cosserat continuum ...

Block 13: Supplementary Note

© 2012 . Published in Granular Matter, Vol. Ed. 0 14, (2) (2012), (, (2). DoD Components reserve a royalty-free, nonexclusive and irrevocable right to reproduce, publish, or otherwise use the work for Federal purposes, and to authorize others to do so (DODGARS §32.36). The views, opinions and/or findings contained in this report are those of the author(s) and should not be construed as an official Department of the Army position, policy or decision, unless so designated by other documentation.

Approved for public release; distribution is unlimited.

Isostaticity in Cosserat continuum

Antoinette Tordesillas · Jingyu Shi · John F. Peters

Received: 29 August 2011 / Published online: 16 March 2012
© Springer-Verlag 2012

Abstract Under conditions of isostaticity in granular media, the contact forces for all particles are statically determinate and forces can be computed without recourse to deformation equations or constitutive relationships. Given that stresses represent spatial averages of inter-particle forces, the stress-equilibrium equations for the isostatic state form a hyperbolic system of partial differential equations that describe the internal stress state using only boundary tractions. In this paper, we consider a Cosserat medium and propose closure relationships in terms of stresses and couple stresses from observations of stress variations in the critical state regime from discrete element simulations and experiments on sand, even though the isostatic condition is only satisfied in an average sense. It is shown that the governing equations are hyperbolic, which can be solved using the method of characteristics. Examples of both analytic and numerical solutions are presented. These examples clearly demonstrate that stress chains (characteristic lines) form oblique angles with the assumed direction of the force chains.

Keywords Isostaticity · Cosserat · Granular · Force chains

1 Introduction

It is well known that in two dimensions the equations for classical plasticity form a hyperbolic system of partial dif-

ferential equations (e.g. [1]). These equations are obtained by rendering the system of momentum balance equations statically determinate via the yield criterion (e.g. Coulomb-Mohr relation in [1]), which provides an additional relationship among stresses necessary to close the system of equations. Thus, the stress in a medium undergoing plastic flow can be computed from the boundary conditions, without recourse to the deformation or stress-strain relationships.

Blumenfeld and co-workers [2–5] examined isostaticity, a state in which the forces are statically determinate for an assembly of rigid particles. Continuum equations derived from this state reflect the conditions at the particle scale and are likewise statically determinate, giving rise to a set of governing equations that are hyperbolic. In reality, all particles possess some compliance, form frictional contacts and, for dense granular materials, are generally hyperstatic in the stable pre-failure regime. The question that then arises is under what states might the condition of statically determinate stresses or isostaticity be reasonably assumed in a continuum as well as at the particle scale? Before proceeding, note that the issue of compliance for frictionless (Hertzian) contact was addressed by Blumenfeld [6]; therein he showed that provided the mean coordination number in d -dimensions is $d + 1$, a macroscopic system of compliant but frictionless particles can be mapped onto an equivalent assembly of perfectly rigid particles that approximately supports the same stress field. The error or discrepancy between the two stress fields decays with system size according to a power law. In this paper, however, we focus on developing a statically determinate set of Cosserat constitutive relations for a granular assembly comprising frictional, compliant particles.

It is instructive to explore the differences and similarities between the system of equations from classical plasticity and those of isostaticity in [2–5]. As in two-dimensional plasticity theory (e.g. [1]), the stress in an isostatic medium can

A. Tordesillas (✉) · J. Shi
Department of Mathematics and Statistics, University of
Melbourne, Parkville, VIC 3010, Australia
e-mail: atordes@ms.unimelb.edu.au

J. F. Peters
US Army Engineer Research and Development Center,
Vicksburg, MS 39180-6199, USA

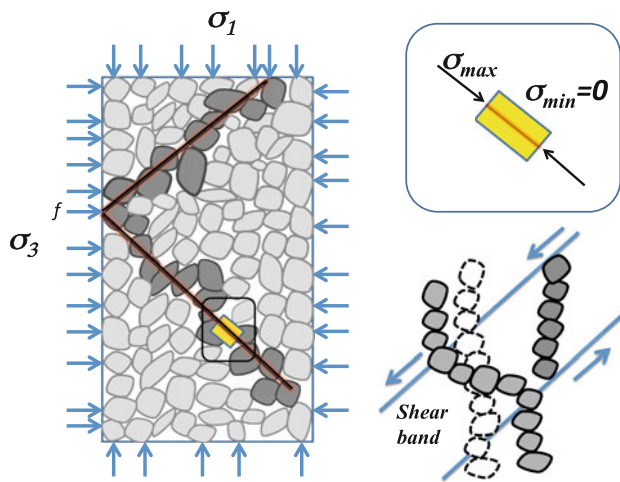


Fig. 1 Stress chains, force chains (*dark gray particles*), and the relationship between stress along a characteristic line and the average stress of the sample volume (*left and top right*). Depiction of a growth and collapse by buckling of force chains in a shear band (*bottom right*): a force chain grows in *upper band* region from a particle chain under compression opposing the shear, while an existing force chain in *lower band* region undergoes buckling with middle segment under extension and rotating in the direction of shear

be found solely from the tractions applied to the boundaries. Thus the key difference between the equations of plasticity and isostaticity lies in the fact that while the former applies only when the continuum is in an ideally plastic state, the latter applies at *all* stress states and for both continuum and particle scales. Another aspect that is common to both systems of equations is their type, i.e. hyperbolic. The physical interpretation of hyperbolic partial differential equations is often built on understanding the characteristics. In plasticity, the characteristics can either be lines in the directions of critical shear stress (stress formulation) or slip lines (kinematic formulation). For plasticity based on an associated flow law, these characteristics are the same, although Spencer [1] describes a “double-shearing” model in which these two characteristics coincide for the case of non-associated flow. The characteristic lines in [2–5] are interpreted as “stress chains”, the directions of which are determined by a local fabric tensor that arises naturally from their analysis. If the definition of stress chain is extended to mean a characteristic trajectory along which a particular stress state is computed, the characteristics of limit plasticity and of media in the isostatic state (e.g. [2–5]) can both be thought of as stress chains. Indeed if the boundary conditions causing stress chains in the analysis by [2–5] are applied to a medium at the plastic limit state, stress chains are likewise produced. Therefore, stress chains arise because the continuum equations are of hyperbolic type.

To what extent then are stress chains similar to the force chains observed in discrete element simulations of granular materials (e.g. [7]) and experiments with photoelastic disks

(see [8,9])? Here the relationship between the directions of the characteristics and those of the principal stress warrants attention. Consider the biaxial test wherein the principal axes remain parallel to the sides of the specimen. Characteristics that define stress chains propagate at oblique angles relative to the specimen sides to straddle a “cone of influence” [5]. Yet, as shown in [5], the principal axes align locally with the direction of the stress chains. The situation is illustrated in Fig. 1. Here, a boundary load f , acting on a boundary particle, results in the formation of major load-bearing particles arranged in a quasi-linear fashion, i.e. the force chains (dark shaded particles in Fig. 1). The lines correspond to the stress chains or characteristics computed from the continuum equations. Similar chains can be conceived emanating from all boundary forces, from which the average stress is computed. The top right inset in Fig. 1 shows the stress propagated along the stress chain, where it is seen that the local principal stress axis is aligned with the stress chain direction. This correspondence is consistent with the algorithm used to determine if a particle belongs to a particular force chain (e.g. [10]). On the other hand, the principal axes of the average stress state, determined by integrating the boundary forces, is aligned with the specimen boundaries. As such, the principal axes determined from the average stress need not correspond to the local principal stress axes observed by following a particular stress chain.

In a similar vein, an important difference between stress chains and force chains is that a stress chain emanates from a boundary load along which the stress in the interior caused by that load can be determined. However, multiple stress chains can pass through an interior point giving rise to a stress state that is a combination of all intersecting stress chains. In contrast, the average stresses within particles comprising a force chain are the result of the total loads on the system; strictly speaking the *stresses* within the particles cannot be propagated from a particular force, either on the boundary or within the interior.

To resolve the issue of whether stress/force chains follow the material fabric or, as observed in experiments, align with the principal stress axis, it is useful to consider what controls fabric. Like other fabric tensors used in granular mechanics, the fabric tensor of [2–5] is a measure of the relative position of grains and arises naturally from their analysis of isostatic states. In the analysis, the particle assemblage is partitioned into particle groups that surround voids. However there are differences between the fabric tensor in [2–5] and those typically found in the micromechanics literature. In [2–5], the balance of forces and moments gives rise to a closure equation expressed in terms of stresses and elements of the fabric tensor. By contrast, the appellation fabric tensor is often applied to the symmetric tensor created by averaging the outer products of the contact normals. This definition implies a central reference particle and its nearest neighbors

and is for the purposes of describing the extent to which this arrangement is isotropic. The change in either measure of fabric implies a change in the contact topology which, in turn, leads to irreversible (plastic) strains.

Experiments show that under monotonic loading in the biaxial test, the principal axes of the fabric tensor align with the principal axes of stress as do the force chain directions [7,9,11]. If force chains and stress chains are controlled by fabric, how is the observed relationship between force chains and principal stress axes [11] explained? The fabric tensor is presumably related to stress history rather than stress. From experimental soil mechanics, it has been observed that large plastic strains occur with the rotation of principal axes [12], suggesting that the soil fabric rapidly adjusts to the prevailing principal stress directions. The characteristic lines should therefore be related to the stress tensor as well as the fabric tensor, to the extent that the principal axes of each coincide.

A previous paper [13] explored the proposal that stresses in granular media are in fact carried by a “strong contact network” that is almost isostatic but which is embedded within the overall redundantly constrained (hyperstatic or statically indeterminate) particle system. In such systems, however, the very existence of the “strong contact network” is heavily dependent on the “weak contact network”; the latter provides the necessary confining support to enable the build-up of force along particle chains that then result in the formation of the former. In studies of initially isotropic systems in 2D and 3D, force chains have been observed to develop along chains of particles with a higher degree of redundancy (hyperstatic)—specifically through supporting contacts in 3-cycle formations [14,15].

In this paper, we advance the investigation in [13–15] and the Cosserat constitutive model in [16] by considering the conditions within shear bands that produce a statically determinate system of continuum equations, even though the conditions at the particle scale are not necessarily isostatic. Consistent with the relatively high porosities found in shear bands in sand [8,11,17,18], idealized assemblies in photoelastic disk experiments [9,11], and discrete element simulations [7,14] also exhibit low average coordination number per particle in shear bands compared to the rest of the sample, although this quantity is observed to fluctuate in the band both spatially and temporally [7,9,14]. The rises and falls in the average coordination number—in both space and time—are due to the continual process of creation of new, and collapse by buckling of old force chains, as illustrated in Fig. 1 (bottom right). Corroborative evidence from high resolution experiments on sand [17,18] suggest that regions of high (hyperstatic) and low (isostatic/hypostatic) coordination numbers alternate spatially along the band, with the former being jamming zones where force chains grow and the latter being unjamming zones where force chains collapse by buckling. The relative dominance of these two compet-

ing events of jamming and unjamming determines which of the elastic rises and unstable drops in the strain evolution of the macroscopic stress occur [19]. Thus, in the so-called critical state regime wherein the equations of limit plasticity hold, and for which the sample deforms in the presence of fully developed shear bands, static determinacy in the continuum stresses results from both spatial and temporal averaging of the stress of their particulate counterparts. Accordingly, this study explores conditions of isostaticity for a Cosserat medium based on observations of stresses in the critical state in a manner consistent with the recent analysis of confined force chain buckling in [16,20].

The rest of the paper is arranged as follows. A set of closure relations for an isostatic Cosserat medium is presented in Sect. 2 with analytical solutions in Sect. 3 for the special case where stress characteristics are straight lines. A numerical scheme for more general cases with an example is shown in Sect. 4. To the extent possible, comparisons are made with the analysis put forth in Gerritsen et al. [5]. Concluding remarks are given in Sect. 5.

2 Closures for isostatic Cosserat continuum

We explore isostatic conditions achieved, on average, in space and time, through the collective birth and death of force chains [7,8,11,18,19]. We consider a set of closure relations which, when combined with the momentum balance relations for a Cosserat continuum, lead to a statically determinate system of equations. There are six unknown stress components: 4 for stress and 2 for couple stress. With three equilibrium equations, three relations for the stresses are needed.

Closure I—relation between normal stresses: A defining aspect of the large strain, fully developed plastic flow regime, or “critical state”, for granular materials undergoing localized failure—is the almost steady evolution with strain of the shear stress expressed through the stress ratio $(\sigma_{11} - \sigma_{22})/(\sigma_{11} + \sigma_{22})$. The continual growth of new force chains amidst collapse by buckling of old force chains in the persistent shear band is believed to be the mechanism underpinning this trend [7,8,11,17–20]. Hence we propose the closure relation:

$$\sigma_{22} = G\sigma_{11}. \quad (1)$$

This proportionality relation is of the same form as that derived from the force chain buckling analysis in [20].

Closure II—relation between shear stresses: For a classical continuum, the stresses are symmetric with $\sigma_{12} = \sigma_{21}$. We wish to investigate the influence of asymmetry in the stress tensor, when there is a gradient in moments, which we assume to be small. Thus we propose a simple proportionality between shear stresses for a second closure relation, such that the classical relation $\sigma_{12} = \sigma_{21}$ is recovered when $T = 1$:

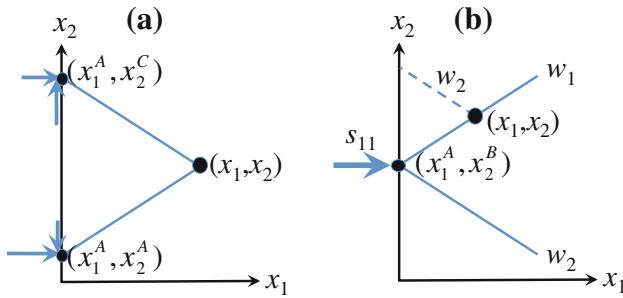


Fig. 2 Illustration of the determination of stresses from characteristics: (a) through a point inside the half plane from two boundary forces, (b) through the point of action of an applied boundary stress

$$\sigma_{12} = T\sigma_{21}. \tag{2}$$

Closure III—relation for couple stresses: A similar proportionality relation as above is proposed:

$$\mu_1 = M\mu_2. \tag{3}$$

The special case of $M = 0$ follows directly from the particle kinematics in the buckling model in [16,20]. Note that a detailed account of this buckling model is given in [20], including a full justification of its assumptions and a comprehensive comparison of its predictions with those observed from: (i) force chain evolution in discrete element simulations and (ii) global trends for stress from experiments on sand.

Equilibrium equations: With the above closure relations, the equilibrium equations for the case of uniform closure coefficients G, T, M become

$$\frac{\partial \sigma_{11}}{\partial x_1} + T \frac{\partial \sigma_{21}}{\partial x_2} = 0, \tag{4}$$

$$\frac{\partial \sigma_{21}}{\partial x_1} + G \frac{\partial \sigma_{11}}{\partial x_2} = 0, \tag{5}$$

$$M \frac{\partial \mu_2}{\partial x_1} + \frac{\partial \mu_2}{\partial x_2} = (T - 1)\sigma_{21}. \tag{6}$$

3 Analytical solutions for Cauchy stresses with straight characteristics

The governing system of equations are (4)–(6): in general $G > 0$ and, for $T > 0$, (4)–(5) are strictly hyperbolic and the influence of an asymmetric stress tensor can be probed for $T > 0$ ($T \neq 1$). Here, we consider the special case $M = 0$, in line with the force chain buckling model in [20]. Equation (6) can be used to determine the couple stress μ_2 , once σ_{21} is established from (4)–(5). In cases of constant coefficients G and T , and hence constant GT , the characteristics comprise two families of straight parallel lines, w_1 and w_2 , with slopes $\pm\lambda = \pm\sqrt{GT}$. Along these characteristics

lines, stresses are constant. We use solutions to these cases to test the numerical scheme needed to solve more complex boundary value problems (next section). The boundary conditions for the two cases below are: (1) two concentrated forces act at points (x_1^A, x_2^A) and (x_1^A, x_2^C) (Fig. 2a), and (2) a concentrated normal force $\sigma_{11} = s_{11}$ acts at point (x_1^A, x_2^B) (Fig. 2b).

In case 1, two characteristic lines from the points of action of the concentrated forces at the boundary intersect at (x_1, x_2) . The stresses $\sigma_{11}(x_1, x_2)$ and $\sigma_{21}(x_1, x_2)$ can be obtained in terms of the applied concentrated forces at the boundary, keeping in mind these have normal and shear components. Along the w_1 characteristic from the point (x_1^A, x_2^A) , we have

$$\lambda\sigma_{11}(x_1, x_2) + \sigma_{21}(x_1, x_2) = \lambda\sigma_{11}(x_1^A, x_2^A) + \sigma_{21}(x_1^A, x_2^A).$$

Along the w_2 characteristic from the point (x_1^A, x_2^C) ,

$$\lambda\sigma_{11}(x_1, x_2) - \sigma_{21}(x_1, x_2) = \lambda\sigma_{11}(x_1^A, x_2^C) - \sigma_{21}(x_1^A, x_2^C).$$

In case 2, the stresses are zero except for the points along the pair of characteristics passing through (x_1^A, x_2^B) : the w_1 characteristic is $x_2 = x_2^B + \lambda(x_1 - x_1^A)$ and the w_2 characteristic is $x_2 = x_2^B - \lambda(x_1 - x_1^A)$. At a point (x_1, x_2) along w_1 , $\lambda\sigma_{11}(x_1, x_2) + \sigma_{21}(x_1, x_2) = \lambda s_{11}$; while $\lambda\sigma_{11}(x_1, x_2) - \sigma_{21}(x_1, x_2) = 0$ along the w_2 characteristic, depicted as a broken line in Fig. 2b. Reminiscent of the so-called stress chains in Gerritsen et al. [4,5], the stresses here are also concentrated along the pair of characteristics through (x_1^A, x_2^B) : $\sigma_{11} = s_{11}/2$ and $\sigma_{21} = \lambda s_{11}/2$ for w_1 , and $\sigma_{11} = s_{11}/2$ and $\sigma_{21} = -\lambda s_{11}/2$ for w_2 .

4 Numerical solutions

If the closure coefficients are general functions $G(x_1, x_2)$, $T(x_1, x_2)$ and $M(x_1, x_2)$, the governing system of equations are coupled and a numerical scheme must be employed. For the constant closure coefficients considered in (4)–(6), the solution scheme proceeds in three steps: first, equations (4) and (5) are solved for σ_{11} and σ_{21} ; second, σ_{22} and σ_{12} are determined from the first two closure relations; and third μ_2 is obtained from (6). Couple stress μ_1 is obtained from the third closure equation (3), but here we focus on the case $M = 0$. Equations (4) and (5) are solved numerically by first approximating the derivatives with respect to x_2 by finite differences; this yields a system of ordinary differential equations with respect to x_1 which is then solved using the 4th-order Runge-Kutta method. We tested this scheme by solving the equations of Gerritsen’s et al. [5]. Two examples are considered for the following region and boundary conditions. The region lies in $0 \leq x_1 \leq 1, 0 \leq x_2 \leq 3$ and is represented by a

uniform mesh of 200 by 600 nodes in the x_1 and x_2 directions, respectively. The boundary conditions on $x_1 = 0$ are: $\mu_1 = 0$ (from the closure relation), $\sigma_{21} = 0$, and the stress σ_{11} is prescribed to be $\sigma_{11} = -20 \text{ N/m}^2$ at node $(x_1, x_2) = (0, 1.5)$, with $\sigma_{11} = -4.0 \text{ N/m}^2$ at two adjacent nodes symmetrically located on either side of node $(0, 1.5)$, and $\sigma_{11} = 0$ for all other points.

Example 1 The uniform closure coefficients are $G = 3$, $T = 1$ and $M = 0$. The resulting characteristic lines have slopes $\sqrt{3}$ and $-\sqrt{3}$, enabling a direct comparison with the analytical solution in Sect. 3. In particular, for the boundary condition $\mu_2 = 0$ on $x_2 = 0$, equation (6) leads to $\mu_2 = 0$ for the whole region which is consistent with the classical continuum case. Further, the results here can be compared with those in Gerritsen et al. [5] for that case when their fabric tensor $p_{11} = 1$, $p_{22} = -3$ and $p_{12} = 0$ (see [5] for the notation). The stress σ_{11} is concentrated along two straight bands, of slopes $\sqrt{3}$ and $-\sqrt{3}$ (similar to the characteristic lines for case 2 in Sect. 3). These bands form an “influence wedge”, reminiscent of the influence cone by Gerritsen [5]. Like the influence cone of Gerritsen et al. [5], we find subregions in the influence wedge in which σ_{11} is nonzero or even positive (i.e. tensile), albeit its magnitude is small. The analytical solution in Sect. 3, however, dictates that the stress inside this influence wedge is zero. We analyzed the sensitivity of the numerical solution to mesh size and found that the magnitude of the stress in these subregions decreases as the mesh size used to approximate the partial derivative with respect to x_2 decreases, suggesting that these tensile stress zones are an artifact of the numerical scheme.

Example 2 In the DEM simulations of [7], the shear stress fluctuates about a near constant value; for the specific system in Fig. 3 of [7], the stress ratio is $(\sigma_{11} - \sigma_{22})/(\sigma_{11} + \sigma_{22}) = 0.35$, i.e. $\sigma_{22} = 2.1\sigma_{11}$. Solutions corresponding to this relation, with $G = 2.1$ and $M = 0$, for the values of $T = 0.5, 1.0, 1.5$ are shown in Figs. 3 and 4: here the nonzero stress inside the influence wedge formed by the characteristics is evident, and most pronounced for $T = 0.5$.

Finally, Gerritsen et al. [4,5] showed that consideration of non-constant closure coefficients lead to “stress leakage”, i.e. non-zero stresses develop inside the influence cone, the magnitude of which depends on the specific form of the closure coefficients. For example, they found that periodically varying closure coefficients lead to a periodic pattern in the stresses, and the two bands of concentrated stress bear a periodic waveform. We also observed stress leakage from consideration of a small variation in our closure coefficients (data not shown).

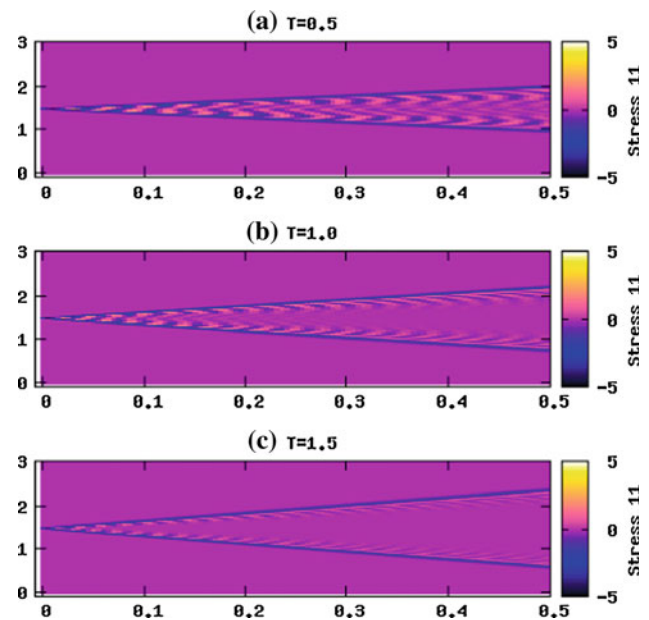


Fig. 3 Distribution of stress component σ_{11} for a constant stress ratio of 0.35 (in accordance with [7]) and **a** $T = 0.5$, **b** $T = 1$, **c** $T = 1.5$

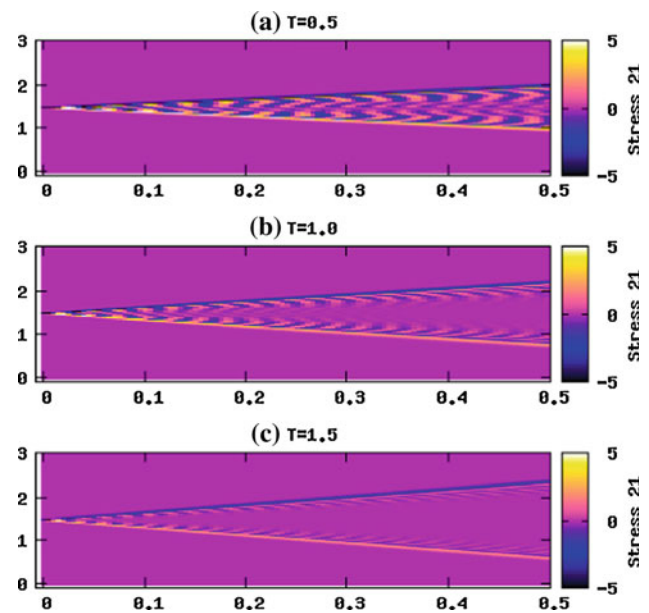


Fig. 4 Distribution of stress component σ_{21} for a constant stress ratio of 0.35 (in accordance with [7]) and **a** $T = 0.5$, **b** $T = 1$, **c** $T = 1.5$

5 Concluding remarks

The static determinacy of granular media in the fully developed plastic or critical state regime is investigated. The predictions of the Cosserat model display many similarities with those arising from the isostatic state investigated by Blumenfeld and co-workers [2–5]. In both cases, when the closure coefficients are constant, the characteristics associated with a boundary force define an influence wedge. Outside the

wedge, the stress is zero; inside the wedge, the stresses are non-zero albeit these decrease in magnitude with decreasing mesh size. We also observed what they referred to as “stress leakage” for non-constant closure coefficients. These similarities mostly result from the governing equations being hyperbolic for both the isostatic state and the critical state; however the physical processes rendering the systems hyperbolic are quite different. In the isostatic case, the system is statically determinate at the particle scale, which makes it possible to develop continuum equations that are statically determinate; at the critical state, statical determinacy of the continuum equations results from the spatial-temporal averaging of forces associated with the concomitant birth, and collapse by buckling, of force chains. The forces in the critical state, at the particulate scale, are not statically determinate. The governing equations for the two cases thus represent different physical processes. Despite the similarity in their characteristic solutions, they differ by their information content. The stress chains produced by the isostatic condition are similar to the force chains seen in granular media. In the case of the former, the stress chain carries information derived entirely from the boundary load from which it emanates. In contrast, a force chain represents the combined result of the boundary force and the loading of all particles incepting the chain. The characteristics associated with the governing equations for the critical state represent the limiting stress state, which is essentially equivalent to the case of limiting plasticity. The stress at the critical state is not necessarily constant but fluctuates, with rises and falls tied to the jamming and unjamming occurring inside the material. The limiting state thus represents a time-averaged quantity.

At the critical state, the stress states are episodic, with rises in stress related to force chain creation (jamming) followed by unstable falls in stress related to force chain buckling (unjamming). This inference on mechanisms associated with jamming-unjamming process comes from direct observations of the shear stress through the stress ratio, extracted from DEM simulations and experiments on photoelastic disk assemblies and on sand [7–9, 11, 14, 17–20]. Likewise, the closure equations used to obtain the governing equations depend, to some extent, on direct observation of how quantities vary in simulations and experiments. Our ultimate goal is to develop a micromechanical model that predicts the above-mentioned observations, based on closure equations that are derived from a combined: (i) stochastic analysis of the birth-death process of an assembly of force chains in distinct stages of buckling, and (ii) a comprehensive structural mechanics model of the different stages in the evolution of a laterally confined force chain under axial compression. This work is underway.

Finally, we close with questions arising from this study. The comparison between particle scale mechanisms and the continuum description produced for the isostatic and criti-

cal states begs the question of how much of the particulate behavior survive the passage to the continuum representation via averaging over the representative volume. In the case of the critical state, is the continuum model even a proper representative of the particulate behavior? Indeed, the averaging of the particulate equations entirely masks the turmoil that actually occurs at the particle scale. Such a difference might be significant if, for example, coupled processes on the mesoscale were under consideration (e.g. soil–water interaction). At variance to classical continua, should the rheology of complex media be formulated at the level of basic units (i.e. particle scale)—prior to averaging to a continuum approximation? If so, what of the interactions between mesoscopic entities made up of the fundamental units (i.e. force chains)? In regard to the continuum equations describing the isostatic state, a similar critical analysis can be made. Each stress chain represents the stress caused by a concentrated load at the specimen boundary. The stress state at any particular point is the result of adding the stresses from the preponderance of stress chains intersecting the point. Therefore, the stress distribution using the hyperbolic governing equations of the isostatic medium is the net result of all boundary forces. For example, even though each stress chain is aligned in the direction of the principal axis caused by the boundary force, it need not be aligned with the principal axis of the total stress at the point. In addition, an increment of load causes rearrangement of particles that is manifest by a strain of the continuum element. Presumably, the stress and strain increment can be related through a constitutive relationship, which when combined with the equations of equilibrium, result in elliptic governing equations. The ability to relate stress and strain does not depend on the specimen being in an isostatic state (with rigid particles) because the strain is caused by relative movements among particles and not the deformation of the particles themselves. It follows that the stress can be determined either by hyperbolic equations or elliptic equations, which in principle should produce the same results.

Acknowledgments We acknowledge the support of the Australian Research Council ARC (DP0986876), the US Army Research Office (W911NF-07-1-0370 & W911NF-11-1-0175) and the Melbourne Energy Institute. AT thanks Raphael Blumenfeld for suggesting an investigation of potential isostatic conditions inside shear bands.

References

1. Spencer, A.J.M.: Double-shearing theory applied to instability and strain localization in granular materials. *J. Eng. Math.* **45**, 55–74 (2003)
2. Blumenfeld, R.: Stresses in isostatic granular systems and emergence of force chains. *Phys. Rev. Lett.* **93**, 108301 (2004)
3. Blumenfeld, R.: Stresses in two-dimensional isostatic granular systems: exact solutions. *New J. Phys.* **9**, 160 (2007)

4. Gerritsen, M., Kreiss, G., Blumenfeld, R.: Stress chain solutions in two-dimensional isostatic granular systems: fabric-dependent paths, leakage, and branching. *Phys. Rev. Lett.* **101**, 098001 (2008)
5. Gerritsen, M., Kreiss, G., Blumenfeld, R.: Analysis of stresses in two-dimensional isostatic granular systems. *Physica A* **387**, 6263–6276 (2008)
6. Blumenfeld, R.: Stress transmission and isostatic states of non-rigid particulate systems. *Modeling Soft Matter IMA Vol. Math. Its Appl.* **141**, 235–246 (2005)
7. Tordesillas, A.: Force chain buckling, unjamming transitions and shear banding in dense granular assemblies. *Phil. Mag.* **87**, 4987–5016 (2007)
8. Oda, M., Konishi, J., Nemat-Nasser, S.: Experimental micromechanical evaluation of strength of granular materials: effects of particle rolling. *Mech. Mater.* **1**, 269–283 (1982)
9. Tordesillas, A., Zhang, J., Behringer, R.P.: Buckling force chains in dense granular assemblies: physical and numerical experiments. *Geomech. Geoeng.* **4**, 3–16 (2009)
10. Peters, J.F., Muthuswamy, M., Wibowo, J., Tordesillas, A.: Characterization of force chains in granular material. *Phys. Rev. E* **72**(4), 041307 (2005)
11. Oda, M., Nemat-Nasser, S., Konishi, J.: Stress-induced anisotropy in granular masses. *Soils Found.* **25**(3), 85–97 (1985)
12. Arthur, J.R.F., Rodriguez del, C.J.I., Dunstan, T., Chua, K.S.: Principal stress rotation: a missing parameter. *J. Geotech. Eng. Div.* **106**(4), 419–433 (1980)
13. Walker, D.M., Tordesillas, A., Thornton, C., Behringer, R.P., Zhang, J., Peters, J.F.: Percolating contact subnetworks on the edge of isostaticity. *Granul. Matter* **13**, 213–240 (2011)
14. Tordesillas, A., O’Sullivan, P., Walker, D.M., Paramitha, S.: Micromechanics of granular materials: evolution of functional connectivity in contact and force chain networks: feature vectors, k-cores and minimal cycles. *Comptes Rendus Mécanique* **338**, 556–569 (2010)
15. Tordesillas, A., Pucilowski, S., Walker, D.M., Peters, J., Hopkins, M.: A complex network analysis of granular fabric in three-dimensions. *Dyn. Continuous, Discret Impuls. Syst. Ser. B.* (in press) (2012)
16. Tordesillas, A., Muthuswamy, M.: A thermomicromechanical approach to multiscale continuum modeling of dense granular materials. *Acta Geotech.* **3**, 225–240 (2008)
17. Oda, M., Takemura, T., Takahashi, M.: Microstructure in shear band observed by microfocus X-ray computed tomography. *Geotechnique* **54**, 539–542 (2004)
18. Rechenmacher, A.L.: Grain-scale processes governing shear band initiation and evolution in sands. *J. Mech. Phys. Solids* **54**, 22–45 (2006)
19. Tordesillas, A., Shi, J., Tshaikiwsky, T.: Stress-dilatancy and force chain evolution. *Int. J. Numer. Anal. Meth. Geomech.* **35**, 264–292 (2011)
20. Tordesillas, A., Muthuswamy, M.: On the modeling of confined buckling of force chains. *J. Mech. Phys. Solids* **57**, 706–727 (2009)